

New Phenolic Glycosides from *Coelogyne fuscescens* Lindl. var. *brunnea* and Their Cytotoxicity against Human Breast Cancer Cells

May Thazin Thant, Narumol Bhummaphan, Jittima Wuttiin, Charoenchai Puttipanyalears, Waraluck Chaichompoo, Pornchai Rojsitthisak, Yanyong Punpreuk, Chotima Böttcher, Kittisak Likhitwitayawuid, and Boonchoo Sritularak*



Cite This: *ACS Omega* 2024, 9, 7679–7691



Read Online

ACCESS |



Metrics & More

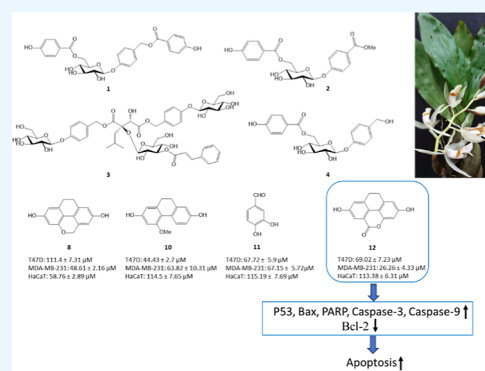


Article Recommendations



Supporting Information

ABSTRACT: The phytochemical investigation of the whole plants of *Coelogyne fuscescens* Lindl. var. *brunnea* led to the discovery of three new phenolic glycosides, i.e., coelofusides A–C (1–3) and 12 known compounds (4–15). For the first time, we reported the nuclear magnetic resonance (NMR) data of 4-*O*-(6'-*O*-glucosyl-4"-hydroxybenzoyl)-4-hydroxybenzyl alcohol (4) in this study. The identification of the structures of newly discovered compounds was done through the analysis of their spectroscopic data [NMR, mass spectrometry, ultraviolet, Fourier transform infrared, optical rotation, and circular dichroism (CD)]. In comparison to anticancer drugs (i.e., etoposide and carboplatin), we evaluated anticancer potential of the isolated compounds on two different breast cancer cell lines, namely, T47D and MDA-MB-231. Human fibroblast HaCaT cells were used as the control cells. After a 48 h incubation, flavidin (8), coelonin (10), 3,4-dihydroxybenzaldehyde (11), and oxoflavidin (12) showed significant cytotoxic effects against breast cancer cells. Among them, oxoflavidin (12) exhibited the most potent cytotoxicity on MDA-MB-231 with an IC₅₀ value of 26.26 ± 4.33 μM. In the nuclear staining assay, oxoflavidin induced apoptosis after 48 h in both T47D and MDA-MB-231 cells in a dose-dependent manner. Furthermore, oxoflavidin upregulated the expression of apoptotic genes, such as p53, Bax, poly(ADP-ribose) polymerase, caspase-3, and caspase-9 genes while significantly decreasing antiapoptotic protein (Bcl-2) expression levels.



INTRODUCTION

Cancer is a complex condition characterized by the abnormal and uncontrolled growth of cells, leading to the formation of a tumor or multiple tumors. Due to its diverse nature and ability to affect various organs and systems in the body, cancer has become a significant cause of mortality worldwide.¹ Breast cancer stands as the most prevalent cancer in women and is ranked as the second leading cause of cancer-related death among women worldwide. In 2020, around 2.3 million new cases were reported, resulting in over 685,000 deaths. It is estimated that the number of new cases of breast cancer will exceed 3 millions with 1 million deaths by the year 2040.² The mortality from breast cancer is exacerbated by the recurrence of the disease, and the disease often becomes resistant to chemotherapy. Thus, there is a pressing need for novel therapeutic drugs for breast cancer. Many anticancer drugs used in clinical settings are derived from natural sources. For instance, vincristine and vinblastine (vinca alkaloids) come from *Catharanthus roseus* L. and paclitaxel (taxane) is derived from *Taxus brevifolia* Nutt. These plant-derived anticancer agents have received clinical approval and are now widely used in cancer treatment.³

The Orchidaceae family is renowned in traditional medicine, particularly in treating infections and tumors.⁴ However, despite

their traditional medicinal uses, there is limited information about their specific chemical composition. Thus, further exploration and investigation of orchids are warranted for the identification of bioactive compounds present in these plants and to assess their potential as sources of novel anticancer agents.^{4,5} In line with our ongoing research on anticancer compounds from orchids,^{6,7} we turned our focus on the *Coelogyne fuscescens* Lindl. var. *brunnea* plant.

C. fuscescens Lindl. var. *brunnea*, belonging to the Orchidaceae family, is recognized as one of the medicinal orchid species with aphrodisiac properties and it is referred to as “Ueang Tian Som” in Thai.⁸ Apart from its medicinal benefits, it is also one of the important ornamental species due to its beautiful flowers and distinctive coconut fragrance.⁹ *C. fuscescens* Lindl. var. *brunnea* possesses a significant value in both horticulture and medicine. Its leaves and pseudobulbs are often applied for therapeutic

Received: September 15, 2023

Revised: January 24, 2024

Accepted: January 26, 2024

Published: February 9, 2024



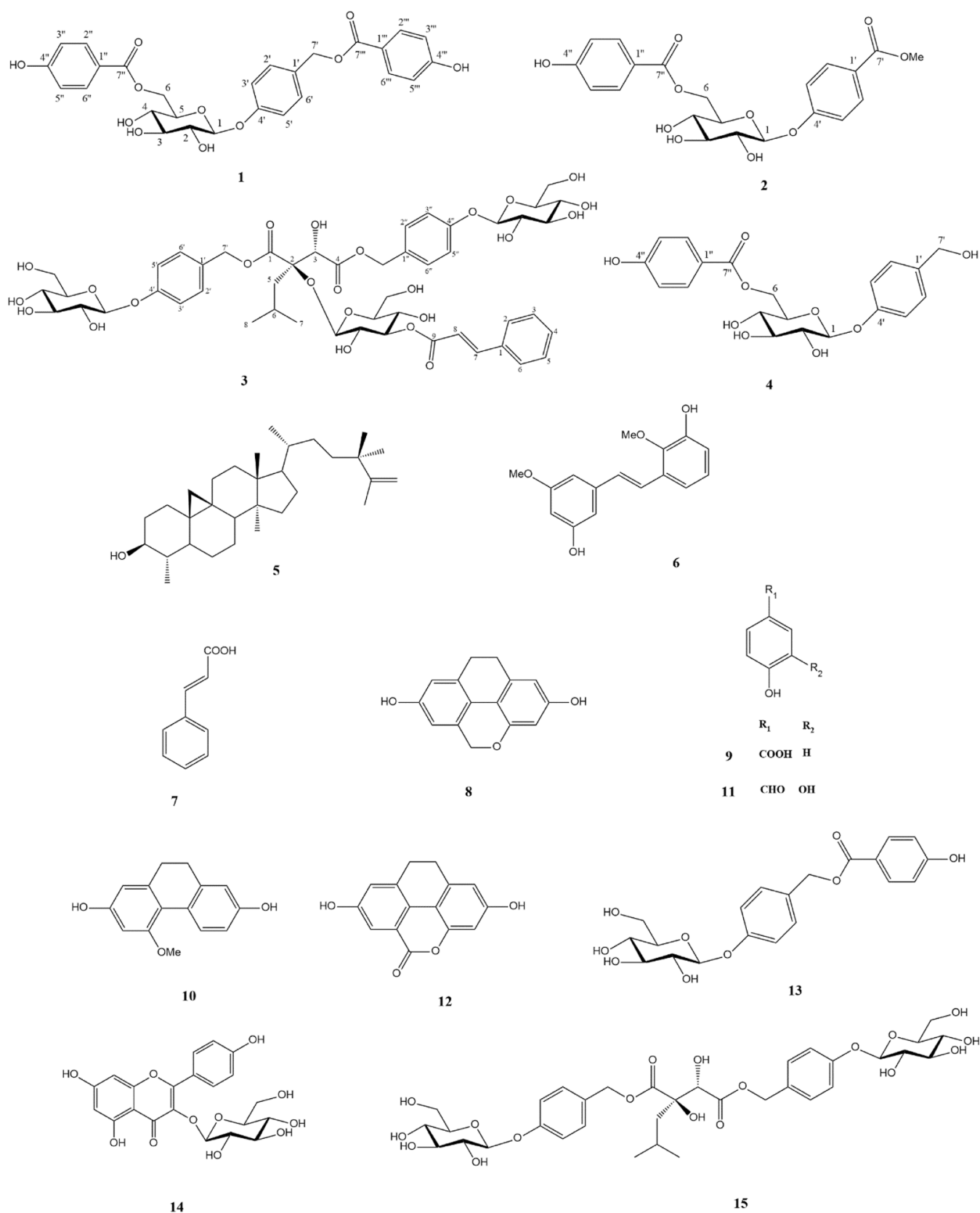


Figure 1. Structures of compounds 1–15 obtained from *C. fuscescens* Lindl. var. *brunnea*.

purposes.¹⁰ The pseudobulb is recognized for various medicinal properties, such as alleviating headaches, fever, abdominal pain, and ear infections. A paste derived from the pseudobulb is also topically used to relieve burned skin.^{9,11} These traditional

applications highlight the therapeutic potential of this plant. However, there is lacking prior information regarding the chemical constituents and a precise evaluation of its therapeutic potential. Our research aims to fill the knowledge gap by

Table 1. ^1H (400 MHz) and ^{13}C NMR (100 MHz) Spectral Data of 1, 2, and 4 in Acetone- d_6

position	1		2		4	
	^1H (multiplicity, J in Hz)	^{13}C , type	^1H (multiplicity, J in Hz)	^{13}C , type	^1H (multiplicity, J in Hz)	^{13}C , type
1	5.06 (d, 7.6)	100.9, CH	5.18 (d, 7.6)	100.2, CH	5.01 (d, 7.6)	101.0, CH
2	3.57 (m)	73.8, CH	3.56 (m)	73.7, CH	3.55 (m)	73.8, CH
3	3.60 (m)	77.1, CH	3.60 (m)	77.0, CH	3.60 (m)	77.1, CH
4	3.53 (m)	70.6, CH	3.55 (m)	70.6, CH	3.53 (m)	70.7, CH
5	3.91 (ddd, 11.6, 9.6, 2.0)	74.3, CH	3.96 (ddd, 9.6, 7.6, 2.0)	74.4, CH	3.89 (ddd, 9.6, 7.6, 2.0)	74.2, CH
6	4.73 (dd, 11.6, 2.0)	63.7, CH ₂	4.73 (dd, 11.6, 2.0)	63.7, CH ₂	4.74 (dd, 11.6, 2.0)	63.8, CH ₂
	4.35 (dd, 11.6, 7.2)		4.35 (dd, 11.6, 7.6)		4.33 (dd, 11.6, 7.6)	
1'		130.4, C		123.8, C		136.2, C
2'	7.37 (d, 8.8)	129.6, CH	7.88 (d, 8.8)	131.1, CH	7.23 (d, 8.8)	127.7, CH
3'	7.12 (d, 8.8)	116.5, CH	7.16 (d, 8.8)	116.0, CH	7.06 (d, 8.8)	116.2, CH
4'		157.7, C		161.3, C		156.8, C
5'	7.12 (d, 8.8)	116.5, CH	7.16 (d, 8.8)	116.0, CH	7.06 (d, 8.8)	116.2, CH
6'	7.37 (d, 8.8)	129.6, CH	7.88 (d, 8.8)	131.1, CH	7.23 (d, 8.8)	127.7, CH
7'	5.25 (s)	65.5, CH ₂		165.9, C	4.56 (s)	63.4, CH ₂
MeO-7'			3.86 (s)	51.2, OCH ₃		
1''		121.5, C		121.5, C		121.6, C
2''	7.95 (d, 8.8)	131.7, CH	7.95 (d, 8.8)	131.7, CH	7.95 (d, 8.8)	131.7, CH
3''	6.97 (d, 8.8)	115.2, CH	6.96 (d, 8.8)	115.2, CH	6.96 (d, 8.8)	115.2, CH
4''		162.0, C		161.9, C		161.9, C
5''	6.97 (d, 8.8)	115.2, CH	6.96 (d, 8.8)	115.2, CH	6.96 (d, 8.8)	115.2, CH
6''	7.95 (d, 8.8)	131.7, CH	7.95 (d, 8.8)	131.7, CH	7.95 (d, 8.8)	131.7, CH
7''		165.5, C		165.4, C		165.5, C
1'''		121.5, C				
2'''	7.90 (d, 8.8)	131.6, CH				
3'''	6.92 (d, 8.8)	115.2, CH				
4'''		161.9, C				
5'''	6.92 (d, 8.8)	115.2, CH				
6'''	7.90 (d, 8.8)	131.6, CH				
7'''		165.6, C				

uncovering potential bioactive compounds and offering insights into the plant's medicinal properties.

In this study, an ethanolic extract of *C. fuscescens* Lindl. var. *brunnea* was fractionated by partitioning between solvents to yield ethyl acetate and aqueous extracts. Both extracts exhibited a notable cytotoxic effect against various cell types and a particular impact on human breast cancer cells, which prompted us to further investigate the specific compounds accountable for the observed cytotoxic activity against breast cancer cells.

RESULTS AND DISCUSSION

Structure Elucidation of Isolated Compounds. Isolation of the ethanol (EtOH) extract of *C. fuscescens* Lindl. var. *brunnea* yielded 15 compounds. Among them, three compounds, coelofusides A–C (1–3), were elucidated as new compounds and 4-*O*-(6'-*O*-glucosyl-4''-hydroxybenzoyl)-4-hydroxybenzyl alcohol (4) was first reported through nuclear magnetic resonance (NMR) analysis. Additionally, 11 known compounds were characterized: cyclopholidonol (5),¹² phoyunbene C (6),¹³ cinnamic acid (7),¹⁴ flavidin (8),¹⁵ *p*-hydroxybenzoic acid (9),¹⁶ coelonin (10),¹⁷ 3,4-dihydroxybenzaldehyde (11),¹⁸ oxoflavidin (12),¹⁹ 4- β -D-glucopyranosyloxybenzyl ester (13),²⁰ kaempferol-3-*O*- β -D-glucopyranoside (14),²¹ and loroglossin (15)²² (Figure 1) (Figures S38–S75).

Compound 1 was isolated as a white, amorphous solid. In high-resolution electrospray ionization-mass spectrometry (HR-ESI-MS), it exhibited a $[\text{M} - \text{H}]^-$ ion peak at m/z : 525.1397 (calcd for $\text{C}_{27}\text{H}_{25}\text{O}_{11}$, 525.1396) (Figure S1). Compound 1 displayed ultraviolet (UV) absorptions at 210 and 255 nm

(Figure S2). The Fourier transform infrared (FT-IR) spectrum showed characteristic absorption bands at 2921 and 1607 cm^{-1} (aromatic ring), 1712 cm^{-1} (C=O), 1513 cm^{-1} (C=C), and 1279 cm^{-1} (C–O) due to the ester carbonyl moiety in addition to strong bands at 3370 cm^{-1} (OH) and 1072 cm^{-1} (C–O), indicating the presence of the sugar moiety²² (Figure S3). The existence of the sugar moiety is also evident in the ^1H NMR (400 MHz) spectra of compound 1 (Table 1). The anomeric sugar proton appeared as a doublet at 5.06 (1H, d, J = 7.6 Hz, H-1), indicating the β -configuration of the glucosyl residue,²² and the other signals of sugar protons exhibited in the range of 3.53–4.73 Hz. The ^{13}C NMR signals (Table 1) were observed for a glucose unit at 100.9 (C-1), 73.8 (C-2), 77.1 (C-3), 70.6 (C-4), 74.3 (C-5), and 63.7 (C-6).¹² The ^1H – ^1H correlation spectroscopy (COSY) spectrum was examined to determine the proton sequence of the initial sugar unit spanning from H-1 to H-6. The ^1H NMR spectrum of compound 1 also revealed six pairs of aromatic signals at δ_{H} 7.37 (2H, d, J = 8.8 Hz, H-2',6'), 7.12 (2H, d, J = 8.8 Hz, H-3',5'), 7.95 (2H, d, J = 8.8 Hz, H-2'',6''), 6.97 (2H, d, J = 8.8, H-3'',5''), 7.90 (2H, d, J = 8.8 Hz, H-2''',6'''), and 6.92 (2H, d, J = 8.8 Hz, H-3''',5'''), demonstrating three 1, 4-disubstituted aromatic rings of two 4-hydroxybenzoic acid moieties¹⁶ and a 4-hydroxybenzyl alcohol group.²⁰ The ester linkage between 4-hydroxybenzoic acid and 4-hydroxybenzyl alcohol was confirmed through a heteronuclear multiple bond correlation (HMBC) cross-peak observed between the methylene protons of the benzyl alcohol moiety δ_{H} 5.25 (2H, s, H-7') and the carbonyl group δ_{C} 165.6 (C-7'''), forming a (4-hydroxyphenyl)methyl 4-hydroxybenzoate structure. The

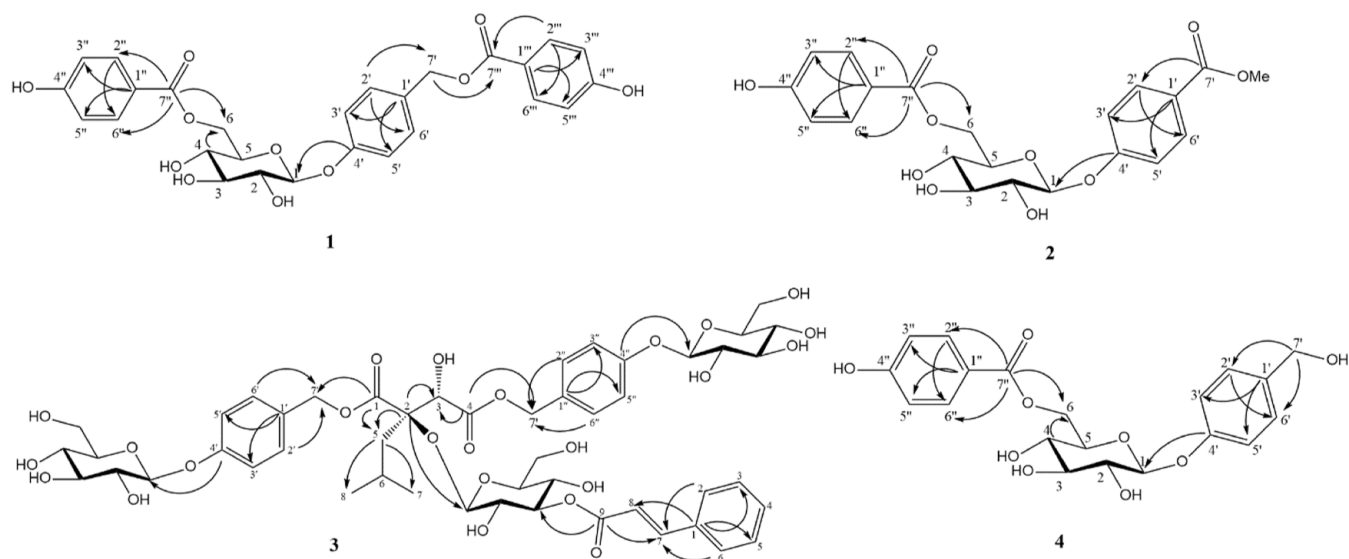


Figure 2. HMBC correlations of **1**, **2**, **3**, and **4**.

HMBC cross-peaks from the anomeric proton of the glucose moiety at δ_{H} 5.06 (1H, d, $J = 7.6$ Hz, H-1) to C-4' of the benzyl alcohol moiety (δ_{C} 157.7) suggested the connection of the (4-hydroxyphenyl)methyl 4-hydroxybenzoate unit at C-1 of glucose. This confirmation was supported by the nuclear overhauser enhancement spectroscopy (NOESY) interactions between the anomeric proton of the glucose moiety and the H-3'/H-5' protons of the benzyl alcohol unit. The second unit of 4-hydroxybenzoic acid was attached at C-6 of glucose via an ester bond, as evidenced by HMBC correlations of H-6 [δ_{H} 4.35 (1H, dd, $J = 11.6, 7.2$ Hz) and 4.73 (1H, dd, $J = 11.6, 2.0$ Hz)] and C-7'' (δ_{C} 165.5) of the benzoyl carbonyl group (Figure 2). Based on the aforementioned data, the structure of compound **1** was demonstrated as shown and given the trivial name coelofuside A (Figures S4–S9).

Compound **2** was isolated as a white, amorphous solid. In HR-ESI-MS, it revealed a $[M - H]^-$ ion peak at m/z : 433.1121 (calcd for $\text{C}_{21}\text{H}_{21}\text{O}_{10}$, 433.1134) (Figure S11). The FT-IR spectrum showed characteristic absorption bands at 2919 and 1610 cm^{-1} (aromatic ring), 1700 cm^{-1} (C=O), 1512 cm^{-1} (C=C), and 1286 cm^{-1} (C–O) due to ester carbonyl group in addition to strong bands at 3353 cm^{-1} (OH) and 1065 cm^{-1} (C–O), indicating the presence of the sugar moiety²² (Figure S12). The compound revealed UV absorptions at 210 and 250 nm (Figure S13). The ^1H NMR spectrum of compound **2** showed four pairs of aromatic signals at δ_{H} 7.88 (2H, d, $J = 8.8$ Hz, H-2',6'), 7.16 (2H, d, $J = 8.8$ Hz, H-3',5'), 7.95 (2H, d, $J = 8.8$ Hz, H-2'',6''), and 6.96 (2H, d, $J = 8.8$ Hz, H-3'',5''), which demonstrated two 1, 4-disubstituted aromatic rings (Table 1). Its ^1H NMR spectrum also exhibited one methoxyl group at δ_{H} 3.86 (3H, s) along with the observation of a methyl ester carbon signals at δ_{C} 165.9 (C-7'') and 51.2 (7'-OMe), indicating the existence of a 4-hydroxy methyl benzoate moiety in compound **2**. Furthermore, the ^1H and ^{13}C NMR data of another 1, 4-disubstituted aromatic ring were consistent with those of 4-hydroxybenzoic acid.¹⁶ The ^1H NMR of compound **2** also showed signals of the glucose moiety (δ 5.18–3.55) with a β -anomeric proton at 5.18 (1H, d, $J = 7.6$ Hz, H-1).²² In the ^{13}C NMR spectrum of compound **2**, a glucosyl unit was observed at δ_{C} 100.2 (C-1), 73.7 (C-2), 77.0 (C-3), 70.6 (C-4), 74.4 (C-5), and 63.7 (C-6).¹² The HMBC correlations between the

anomeric proton signal at δ_{H} 5.18 (1H, d, $J = 7.6$ Hz, H-1) with δ_{C} 161.3 (C-4') supported the linkage of the glucose unit and 4-hydroxy methyl benzoate moiety at C-1 and C-4' by an ether linkage. Similar to compound **1**, 4-hydroxybenzoic acid of compound **2** was positioned at C-6 of the glucose unit, as supported by HMBC correlations of H-6 [δ_{H} 4.35 (1H, dd, $J = 11.6, 7.6$ Hz) and 4.73 (1H, dd, $J = 11.6, 2.0$ Hz)] and C-7'' (δ_{C} 165.4) (Figure 2). Considering the above spectral data, the structure of compound **2** was illustrated as shown and has been named coelofuside B (Figures S14–S18).

Compound **3** was obtained as a white, amorphous solid. In HR-ESI-MS, it revealed a $[M - H]^-$ ion peak at m/z : 1033.3543 (calcd for $\text{C}_{49}\text{H}_{61}\text{O}_{24}$, 1033.3552) (Figure S20). The FT-IR spectrum exhibited absorption bands at 2925 and 1611 cm^{-1} (aromatic ring), 1727 cm^{-1} (C=O), 1512 cm^{-1} (C=C), and 1230 cm^{-1} (C–O) due to ester carbonyl group, gem-dimethyl groups (1386 and 1369 cm^{-1}), and strong broadened absorption band at 3382 cm^{-1} (OH) and 1074 cm^{-1} (C–O), indicating the presence of sugar moieties^{22,23} (Figure S21). Furthermore, compound **3** exhibited UV absorptions of 220, 230, and 275 nm (Figure S22). The ^1H , ^{13}C , and DEPT spectral data (Table 2) of compound **3** exhibited similarities to those of gymnaside IV from *Gymnadenia conopsea* except that the ^1H and ^{13}C NMR data assignable at δ_{H} 4.52 (1H, s, H-3), δ_{C} 74.6 (C-3), and δ_{C} 84.7 (C-2) in compound **3** were shifted downfield compared to that of gymnaside IV [δ_{H} 3.30 (1H, d, $J = 17.7$ Hz, H-3a), 3.46 (1H, d, $J = 17.7$ Hz, H-3b), δ_{C} 42.7 (C-3), and δ_{C} 80.9 (C-2)].²³ These differences indicated the presence of the 2-isobutyltartrate moiety in compound **3** as opposed to the 2-isobutylmalate moiety in gymnaside IV.²⁴

The ^1H NMR spectrum of compound **3** clearly displayed four pairs of overlapped signals at δ_{H} 7.33 (2H, d, $J = 8.8$ Hz, H-2', 6'), δ_{H} 7.30 (2H, d, $J = 8.8$ Hz, H-2'', 6''), 7.14 (2H, d, $J = 8.8$ Hz, H-3', 5'), and 7.11 (2H, d, $J = 8.8$ Hz, H-3'', 5'') and four benzyloxy hydrogens at δ_{H} 5.10 (1H, d, $J = 10.0$ Hz, H-7'a), 4.90 (1H, d, $J = 10.0$ Hz, H-7'b), 5.13 (1H, d, $J = 10.0$ Hz, H-7''a), and 4.96 (1H, d, $J = 10.0$ Hz, H-7''b). The HMBC correlations from H₂-7' to C-1' (δ_{C} 129.0) and C-2'/6' (δ_{C} 130.5) and from H₂-7'' to C-1'' (δ_{C} 128.9) and C-2''/6'' (δ_{C} 130.2) revealed the existence of two 1,4-disubstituted benzylic units in compound **3**. The three anomeric protons at δ_{H} 4.92 (1H, d, $J = 8.0$ Hz, 2-O-

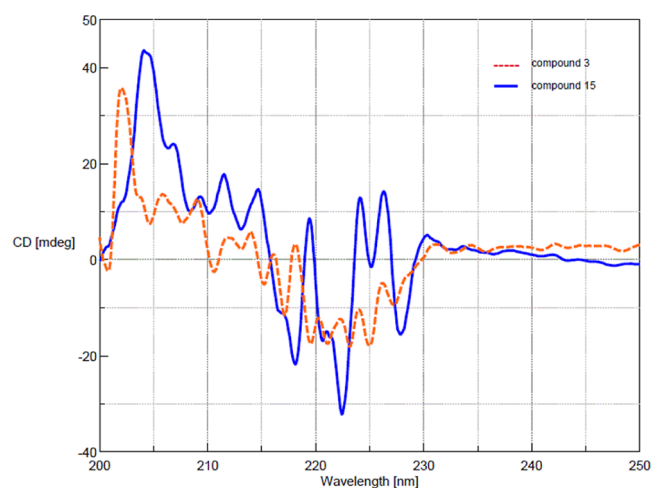
Table 2. ^1H (400 MHz) and ^{13}C NMR (100 MHz) Spectral Data of **3** in Methanol- d_4

position	^1H (multiplicity, J in Hz)	^{13}C , type
1		172.1, C
2		84.7, C
3	4.52 (s)	74.6, CH
4		170.7, C
5	2.14 (dd, 13.9, 5.5)	45.4, CH_2
	1.73 (m)	
6	1.77 (m)	23.5, CH
7	0.78 (d, 6.8)	22.7, CH_3
8	0.93 (d, 6.8)	23.3, CH_3
1'		129.0, C
2', 6'	7.33 (d, 8.8)	130.5, CH
3', 5'	7.14 (d, 8.8)	116.5, CH
4'		158.2, C
7'	5.10 (d, 10.0)	67.0, CH_2
	4.90 (d, 10.0)	
1''		128.9, C
2'', 6''	7.30 (d, 8.8)	130.2, CH
3'', 5''	7.11 (d, 8.8)	116.5, CH
4''		158.0, C
7''	5.13 (d, 10.0)	67.0, CH_2
	4.96 (d, 10.0)	
2-O-Glc-1	4.92 (d, 8.0)	98.0, CH
2	3.45 (m)	72.5, CH
3	5.00 (dd, 9.6, 9.6)	78.0, CH
4	3.64 (dd, 9.6, 9.6)	66.9, CH
5	2.77 (dt, 9.6, 2.6)	75.6, CH
6	3.67 (2H, m)	59.7, CH_2
Cin-1		134.5, C
Cin-2,6	7.65 (dd, 7.6, 2.0)	127.9, CH
Cin-3,5	7.43 (m)	128.6, CH
Cin-4	7.43 (m)	130.2, CH
Cin-7	7.80 (d, 16.0)	145.1, CH
Cin-8	6.63 (d, 16.0)	117.8, CH
Cin-9		167.0, C
4'-O-Glc-1	4.89 (d, 7.7)	100.9, CH
2	3.47 (m)	73.5, CH
3	3.56 (m)	76.5, CH
4	3.41 (m)	69.9, CH
5	3.46 (m)	76.7, CH
6	3.91 (dd, 12.0, 2.4)	61.1, CH_2
	3.72 (m)	
4''-O-Glc-1	5.02 (d, 7.7)	100.6, CH
2	3.48 (m)	73.5, CH
3	3.57 (m)	76.5, CH
4	3.41 (m)	69.9, CH
5	3.46 (m)	76.7, CH
6	3.91 (dd, 12.0, 2.4)	61.1, CH_2
	3.72 (m)	

Glc-1), 4.89 (1H, d, $J = 7.7$ Hz, 4'-O-Glc-1), and 5.02 (1H, d, $J = 7.7$ Hz, 4''-O-Glc-1) and the signals between δ_{H} 2.77 and 5.00 indicated the presence of three glucosyl units.²⁵ The coupling constants between those anomeric protons in the sugar moieties (7.7 and 8.0 Hz) suggest that they all adopt β -configurations.²² The HMBC correlations from the 4'-O-Glc-1 proton to C-4' (δ_{C} 158.2) and from the 4''-O-Glc-1 proton to C-4'' (δ_{C} 158.0), together with NOESY correlations between the 4'-O-Glc-1 proton and H-3' (H-5') and between the 4''-O-Glc-1 proton and H-3'' (H-5'') indicated the presence of two 4-(β -D-

glucopyranosyloxy)benzyl units.²⁵ The linkage of those two 4-(β -D-glucopyranosyloxy)benzyl units was deduced from the HMBC correlations of H₂-7' and C-1 (δ_{C} 172.1) and between H₂-7'' and C-4 (δ_{C} 170.7).

The overlapped signals of another aromatic ring were also observed at δ_{H} 7.65 (2H, dd, $J = 7.6, 2.0$ Hz, Cin-H-2,6) and 7.43 (3H, m, Cin-H-3,4,5), together with δ_{H} 7.80 (1H, d, $J = 16.0$ Hz, Cin-H-7) and 6.63 (1H, d, $J = 16.0$ Hz, Cin-H-8). The linkage between the aromatic ring and the double bond was discerned through the HMBC correlations of the Cin-7 proton to Cin-2 and Cin-6 carbons (δ_{C} 127.9); the Cin-8 proton to the Cin-1 carbon (δ_{C} 134.5); and Cin-2 and Cin-6 protons to the Cin-7 carbon (δ_{C} 145.1) (Figure 2). Additionally, the existence of the carbonyl carbon at Cin-9 (δ_{C} 167.0) revealed the presence of a (*E*)-cinnamoyl group in compound **3**.²⁵ The 2-O-Glc-3 proton at δ_{H} 5.00 (1H, dd, $J = 9.6, 9.6$ Hz) showed HMBC correlations to the Cin-9 carbon (δ_{C} 167.0), thus delineating the position of the (*E*) cinnamoyloxy group at the 2-O-Glc-3 carbon. Finally, the HMBC correlation from the 2-O-Glc-1 proton to C-2 revealed that the anomeric proton of the 2-O-glucose moiety is connected to a 2-isobutyltartrate unit at C-2. NMR spectral data of compound **3** was similar to those of loroglossin (**15**) obtained from this plant, only differing in extra functional groups at C-2 in compound **3**. Both compounds exhibited similar circular dichroism (CD) properties, demonstrating a positive cotton effect at 200–219 nm and a negative cotton effect at 220–230 nm (Figure 3). The configuration at C-2 and C-3 of the 2-

**Figure 3.** CD spectra of compounds **3** and **15**.

isobutyltartrate structure was characterized as 2R and 3S by comparing its specific rotation, CD spectra, and NMR data with loroglossin (**15**)²² (Figures S23–S27). Loroglossin is the most commonly known orchid glucoside isolated from several orchid species such as *Orchis latifolia* Linn., *Dactylorhiza hatagirea* D. Don., and *Habenaria petalodes* Lindl.^{22,26,27} Therefore, it was concluded that compound **3** had a structure as established, and the trivial name coelofuside C was given to the compound.

Compound **4** was isolated as a white, amorphous solid. In HR-ESI-MS, it revealed a $[\text{M} - \text{H}]^-$ ion peak at m/z : 405.1176 (calcd for $\text{C}_{20}\text{H}_{21}\text{O}_9$, 405.1185) (Figure S28). The FT-IR spectrum displayed characteristic absorption bands at 2919 and 1608 cm^{-1} (aromatic ring), 1513 ($\text{C}=\text{C}$), 1700 cm^{-1} ($\text{C}=\text{O}$), and 1284 cm^{-1} ($\text{C}-\text{O}$) due to ester carbonyl functions in addition to strong absorption bands at 3347 cm^{-1} (OH) and 1071 ($\text{C}-\text{O}$) cm^{-1} , indicating the presence of the sugar

moiety²² (Figure S29). In the UV spectrum of compound 4, absorptions were comparable to those of compounds 1 and 2 exhibiting the UV absorptions at 210, 230, 260, and 314 nm (Figure S30). From the ¹H NMR (400 MHz) spectra of compound 3, the anomeric sugar proton appeared at δ_{H} 5.01 (1H, d, $J = 7.6$ Hz, H-1) and other signals of sugar protons around 3.53–4.74 ppm (Table 1). Other substituents included a 4-hydroxybenzyl alcohol group [δ_{H} 7.06 (2H, d, $J = 8.8$ Hz, H-3', H-5'), 7.23 (2H, d, $J = 8.8$ Hz, H-2', H-6'), and 4.56 (2H, s, H-7')] and a 4-hydroxybenzoic acid group [δ_{H} 7.95 (2H, d, $J = 8.8$ Hz, H-2'', H-6'') and 6.96 (2H, d, $J = 8.8$ Hz, H-3'', H-5'')]. HMBC correlations were observed between the H-1 of glucose and the C-4' of the 4-hydroxybenzyl alcohol residue which revealed that the glucosidic bond is between C-4' and C-1. The HMBC correlations were also observed between the benzoyl carbonyl group (δ_{C} 165.5) and the methylene protons (H-6) of the glucose residue [δ_{H} 4.33 (1H, dd, $J = 11.6, 7.6$ Hz) and 4.74 (1H, dd, $J = 11.6, 2.0$ Hz)] (Figure 2). Based on the provided spectral data, compound 4 was identified as 4-O-(6'-O-glucosyl-4''-hydroxybenzoyl)-4-hydroxybenzyl alcohol. Compound 4 was previously reported from *Lagenaria siceraria* Stand (bottle gourd) fruit using liquid chromatography–tandem mass spectrometry without NMR data.²⁸ Therefore, this is the first report of NMR data on this compound (Figures S31–S36).

Cytotoxicity of Ethyl Acetate and Aqueous Extracts of *C. fuscescens* Lindl. var. *brunnea* on Prostate Cancer (PC3), Breast Cancer (T47D and MDA-MB-231), Cervical Cancer (SIHA), Colon Cancer (SW620), and Human Fibroblast (HaCaT) Cells. Six different concentrations (0–500 $\mu\text{g}/\text{mL}$) of ethyl acetate and the aqueous extracts of *C. fuscescens* Lindl. var. *brunnea* were screened for cytotoxicity against prostate cancer (PC3), breast cancer (T47D and MDA-MB-231), cervical cancer (SIHA), colon cancer (SW620), and human fibroblast (HaCaT) cells. Both extracts demonstrated notable cytotoxic effects against various cancer cell lines at concentrations of 125, 250, and 500 $\mu\text{g}/\text{mL}$, with cell viability ranging from 10 to 80%. For the breast cancer cells (T47D and MDA-MB-231), both ethyl acetate and aqueous extracts reduced cell viability ($\leq 50\%$) at 125 $\mu\text{g}/\text{mL}$. The IC_{50} values for both extracts against breast cancer cells are detailed in Table 3. In this study, dimethylsulfoxide (DMSO) was employed as a

Table 3. IC_{50} Values of the Aqueous and Ethyl Acetate Extracts of *C. fuscescens* Lindl. *brunnea* against the T47D and MDA-MB-231 Breast Cancer Cell Lines and the HaCaT Human Keratinocyte Cell Line

extracts	cytotoxicity $\text{IC}_{50} \pm \text{SD}$ ($\mu\text{g}/\text{mL}$)		
	T47D	MDA-MB-231	HaCaT
aqueous extract	138.30 \pm 3.15	96.62 \pm 5.48	106.30 \pm 8.41
ethyl acetate extract	125.80 \pm 9.41	116.90 \pm 6.95	74.78 \pm 6.37

negative control to demonstrate that DMSO alone did not influence cell viability compared with the untreated controls (Figure 4).

Cytotoxicity of Isolated Compounds from *C. fuscescens* Lindl. var. *brunnea* on Breast Cancer Cells. Two breast cancer cell lines, T47D and MDA-MB-231, were chosen for further evaluation due to their superior cytotoxic effects over other cell lines. In this study, the cytotoxic effects of isolated compounds (1 and 3–15) were tested at six different concentrations (0–200 μM) (Figure 5). Compound 2 was excluded from evaluation due to its limited quantity.

Carboplatin and etoposide, known chemotherapeutic drugs for breast cancer, were employed as positive controls. Carboplatin, a platinum analogue with single-agent activity, is used to treat advanced-stage breast cancer.²⁹ Previous research has indicated that oral etoposide is a reliable and secure choice for pretreated metastatic breast cancer patients.³⁰ Notably, compounds 8, 10, 11, and 12 revealed significant cytotoxic effects against breast cancer cells, outperforming both etoposide and carboplatin. Compound 8 had IC_{50} values for T47D and MDA-MB-231 at 111.40 ± 7.31 and 48.61 ± 2.16 μM , respectively (Table S1). Additionally, Compound 8 demonstrated greater selectivity toward breast cancer cells over human fibroblasts compared to etoposide, as supported by the IC_{50} values of compound 8 at 58.76 ± 2.89 μM and etoposide at 4.86 ± 0.35 μM . Compound 10 exhibited significant cytotoxicity on T47D and MDA-MB-231 with IC_{50} values of 44.43 ± 2.7 and 63.82 ± 10.31 μM , respectively, while IC_{50} values of the cytotoxic effect on human fibroblasts were 114.5 ± 7.65 μM . The IC_{50} values of compound 11 on T47D, MDA-MB-231, and HaCaT were 67.72 ± 5.9 , 67.15 ± 5.72 , and 115.19 ± 7.69 μM , respectively. Although compound 11 (3,4-dihydroxy benzaldehyde) has been previously investigated for its cytotoxic effects on MCF-7 and MDA-MB-231 breast cancer cells, 0–100 μM did not show an anticancer effect.³¹ Compound 12 exhibited IC_{50} values of 69.02 ± 7.23 and 26.26 ± 4.33 μM on T47D and MDA-MB-231, respectively, surpassing the effects of both etoposide and carboplatin. Compound 12 showed a more potent cytotoxic effect on MDA-MB-231 than all test compounds, etoposide and carboplatin. Moreover, compound 12 was less toxic to human fibroblasts with an IC_{50} value of 113.38 ± 6.31 μM compared to etoposide. The cytotoxicity results of etoposide indicated that it was particularly harmful to human fibroblasts, which are considered as normal human cells, while carboplatin showed a lesser cytotoxic effect on breast cancer cells. Taken together, compounds 8, 10, 11, and 12 revealed superior cytotoxic effects on breast cancer cells compared to carboplatin and less cytotoxicity on human fibroblasts than etoposide.

Oxoflavin Induces Apoptosis in Breast Cancer Cells.

Among the test compounds, compound 12 (oxoflavin) significantly showed a cytotoxic effect on breast cancer cells especially on MDA-MB-231 with an IC_{50} value (26.26 ± 4.33 μM). Moreover, compound 12 has not been previously reported for its anticancer effect on breast cancer cells. Therefore, compound 12 was selected for further investigation of its basic mechanism. Antiproliferative effects of compound 12 showed the highest efficacy in inhibiting cell survival in breast cancer T47D and MDA-MB-231 cell lines. The cytotoxic assay revealed that compound 12 inhibited proliferation in a dose-dependent manner after being treated for 48 h and induced growth inhibition through apoptosis. Compound 12 induced apoptosis in both T47D and MDA-MB-231 cells, as determined by Hoechst/propidium iodide (PI) staining in a dose-dependent manner. It was found that compound 12 stimulated apoptosis and cell death. The cell morphology was observed using a fluorescent microscope. There was shrinkage of an aneurysmal cell wall and a breakdown of DNA, while a concentration of 200 μM induced apoptosis together with necrosis (Figure 6).

Further studies were conducted at the relevant molecular level. Quantitative real-time polymerase chain reaction (qRT-PCR) analysis was employed to determine the impact of compound 12 on the expression of the Bcl-2 gene in human breast cancer cells. MDA-MB-231 cells were treated with

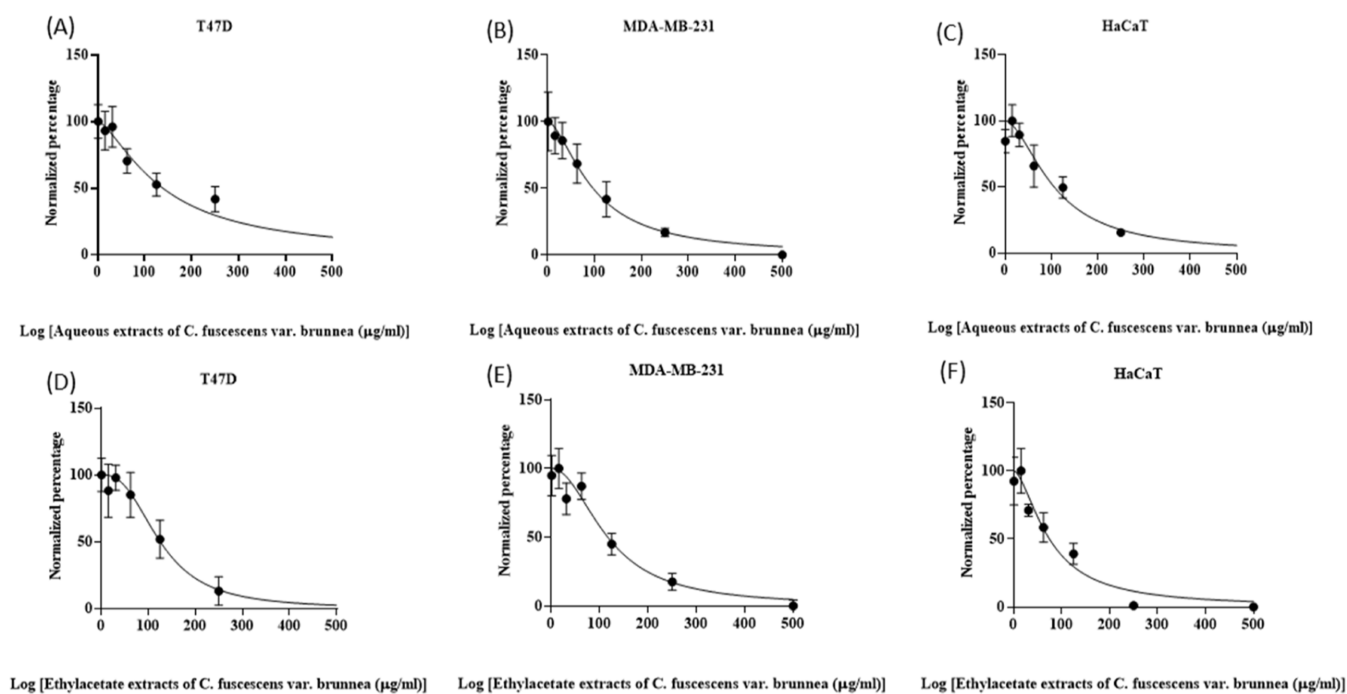


Figure 4. Cytotoxicity effects of the aqueous (A–C) and ethyl acetate extracts (D–F) of *C. fuscescens* Lindl. var. *brunnea* on the T47D and MDA-MB-231 breast cancer cell lines and on the HaCaT human keratinocyte cell line.

compound **12** at 0–25 μM (IC_{50}). The results showed that there was a decrease in Bcl-2 gene expression significantly compared to control cells that were not treated. It was also found that the expression of p53, Bax, poly(ADP-ribose) polymerase (PARP), caspase-3, and caspase-9 genes was markedly elevated in MDA-MB-231 cells following treatment with compound **12** (Figure 7).

The tumor suppressor gene p53 performs a crucial role in different forms of cell death. p53 can selectively trigger apoptosis in tumor cells while causing temporary halting of the cell cycle in normal cells.³² PARP is among the initial cellular proteins identified as a caspase substrate. It undergoes cleavage during the posterior stages of apoptosis and is a focus of numerous chemotherapeutic drugs due to its role as a crucial death substrate.³³ The activation of caspase-3 is pivotal in the apoptotic machinery, serving as a key marker for apoptosis induced by different mechanisms. Previous result demonstrated that apoptosis was triggered in MCF-7 human breast cancer cells via increasing caspase (–3 and –9) activity.³⁴ Caspase-9 is triggered early in the apoptotic process, prompted by the liberation of cytochrome c from the mitochondria in reaction with apoptotic signals. Once activated, caspase-9 initiates the proteolytic activity of subsequent stages of caspases, including caspase-3. The initiation of caspase-3 leads to the fragmentation of crucial cellular components, such as PARP.³⁵ The expression level of Bax is also a crucial indicator for detecting apoptotic cell death. Certainly, the mechanism of apoptosis hinges significantly on the pro-apoptotic (Bax) and antiapoptotic (Bcl-2) proteins.³⁶

In our study, increasing levels of p53, caspase-3, caspase-9, Bax, and PARP while diminishing levels of Bcl-2 play a pivotal role in enhancing the cell's vulnerability to apoptosis by compound **12**.

CONCLUSIONS

In this investigation, 15 compounds were isolated from entire plants of *C. fuscescens* Lindl. var. *brunnea*, consisting of three new phenolic glycosides named coelofusides A–C (1–3) and 12 known compounds (4–15). The NMR data for 4-*O*-(6'-*O*-glucosyl-4''-hydroxybenzoyl)-4-hydroxybenzyl alcohol (**4**) were reported for the first time in this study. This research demonstrated that both ethyl acetate and aqueous extracts of *C. fuscescens* var. *brunnea* showed potential cytotoxic activity against human breast cancer cells T47D and MDA-MB-231. Compounds (**1**, **3**–**15**) were analyzed concurrently, and compounds **8**, **10**, **11**, and **12** exhibited significant anticancer effects on T47D and MDA-MB-231 when compared to anticancer drugs (etoposide and carboplatin). Oxoflavadin (**12**) displayed the most potent cytotoxicity on MDA-MB-231 with an IC_{50} value of $26.26 \pm 4.33 \mu\text{M}$. The assessment of its capability to hinder cell proliferation and induce apoptosis in human breast cancer cell lines was conducted through 3- (4,5-dimethylthiazol-2-yl)-2,5-diphenyltetrazolium bromide (MTT) assay, Hoechst/PI staining, and quantitative RT-PCR analysis. Our findings indicate that the bioactive compounds present in *C. fuscescens* Lindl. var. *brunnea* hold potential as anticancer agents for treating human breast cancer. Compound **12** might serve as a promising candidate for the advancement of effective anticancer drugs for targeting breast cancer.

EXPERIMENTAL SECTION

General Experimental Procedures. Optical rotation was determined by a Jasco P-2000 digital polarimeter (Easton, MD, USA). UV spectra were recorded with a Milton Roy Spectronic 3000 Array spectrophotometer (Rochester, Monroe, NY, USA). CD spectra were obtained from a Jasco J-815 CD spectrophotometer (Hachioji, Tokyo, Japan). FT-IR spectra were measured with a PerkinElmer FT-IR 1760X spectrophotometer (Boston, MA, USA). The Bruker MicroTOF mass spectrometer

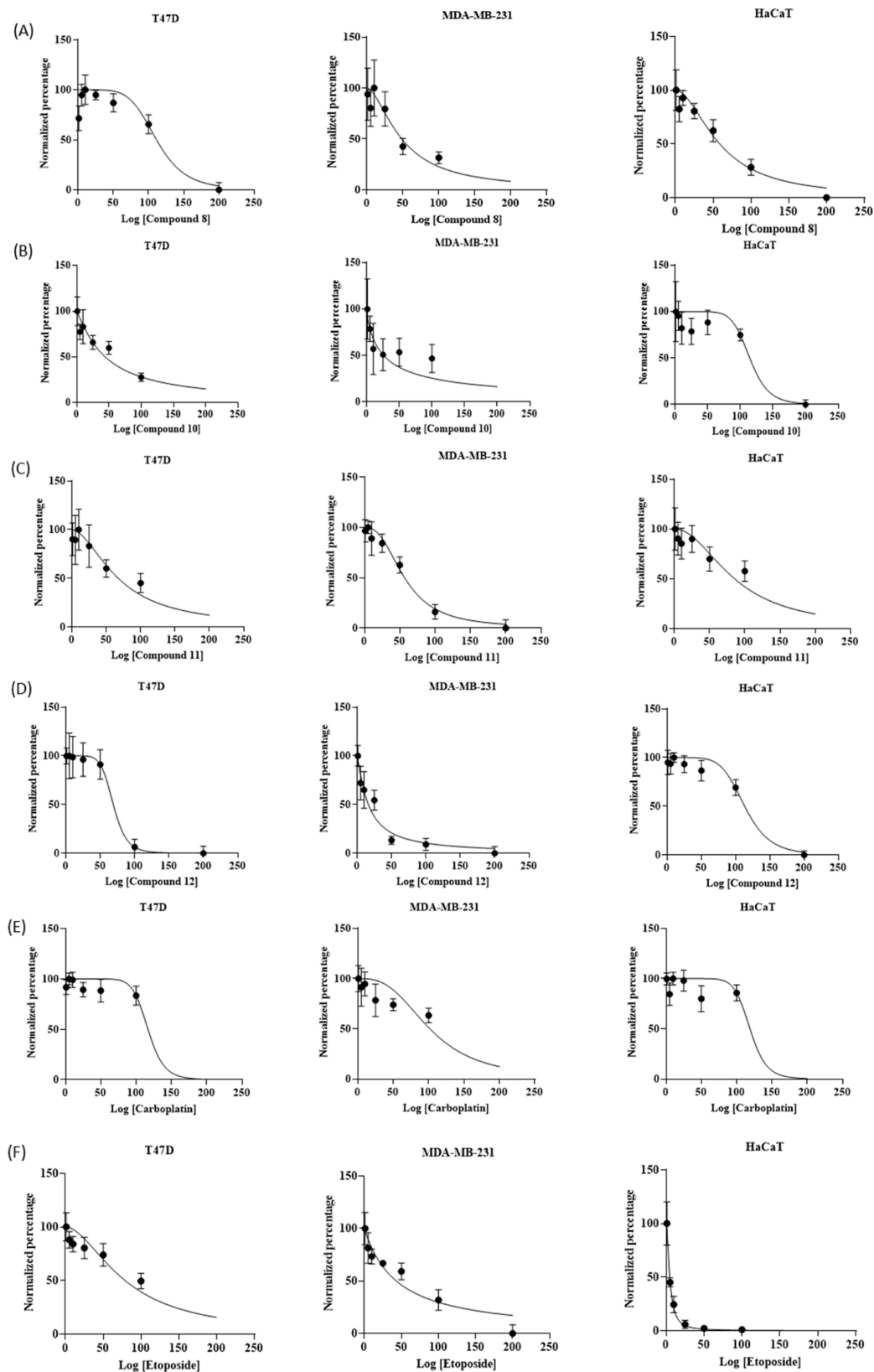


Figure 5. Cytotoxicity effects of compounds 8 (A), 10 (B), 11 (C), 12 (D), carboplatin (E), and etoposide (F) against the T47D and MDA-MB-231 breast cancer cell lines and the HaCaT human keratinocyte cell line.

(ESI-MS) (Billerica, MA, USA) was used to measure mass spectra. NMR spectra were carried through a Bruker Avance Neo 400 MHz NMR spectrometer (Billerica, MA, USA). Semipreparative high-performance liquid chromatography

(HPLC) was conducted using the Shimadzu HPLC (Kyoto, Japan). Chromatography was conducted by silica gel 60 (no. 1.07734.2500), size 0.063–0.200 mm and (no. 1.09385.2500), size 0.040–0.063 mm (Merck, NJ, USA). Reverse-phase column

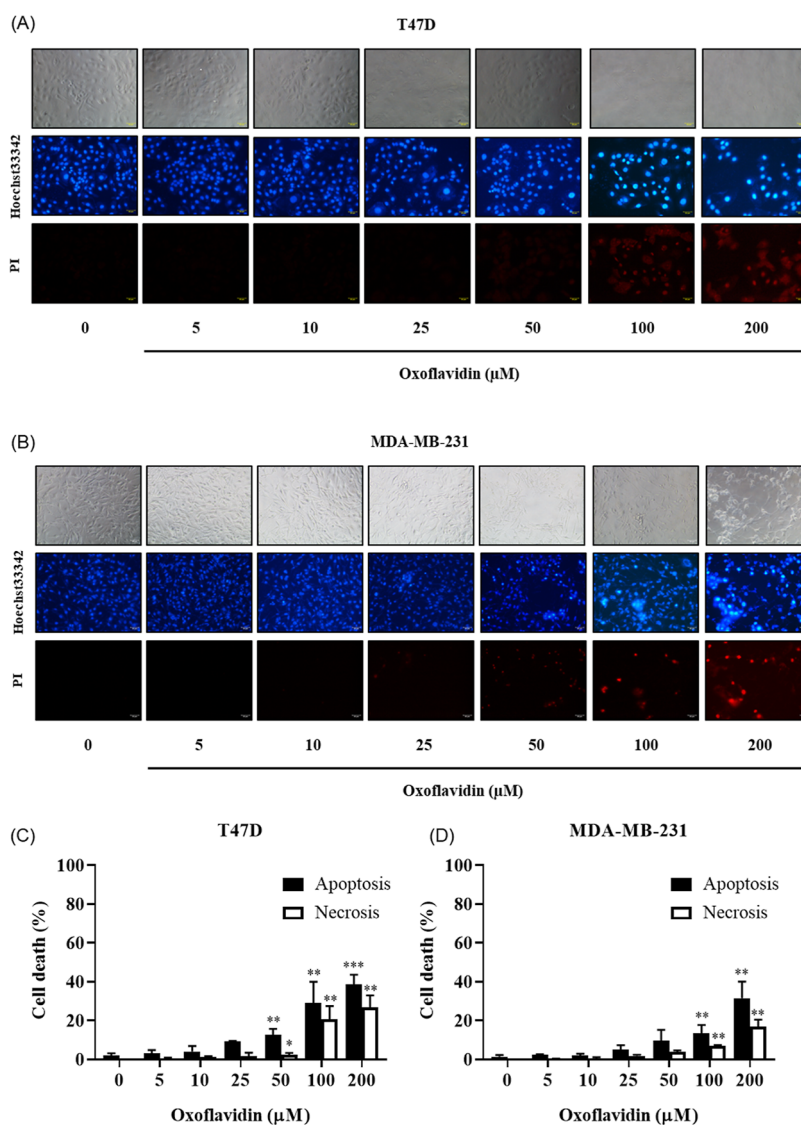


Figure 6. Treatment with compound 12 for 48 h cause apoptosis in both T47D (A) and MDA-MB-231(B) cells in a dose-dependent manner detected via Hoechst33342/PI staining and the percentages of apoptotic and necrotic cell death in T47D (C) and MDA-MB-231 (D) were calculated. Data is represented as the mean \pm SD ($n = 3$) shown in common superscript as * $p \leq 0.05$, ** $p \leq 0.01$, and *** $p \leq 0.001$.

chromatography was done by RP-18 (no. 1.13900.1000), size 40–63 μm (Merck KGaA, Darmstadt, Germany). Sephadex LH-20 (Merck, NJ, USA) was also used for the isolation of compounds. Diaion HP-20 column chromatography was performed on polar copolymer styrene-divinylbenzene adsorbent resin with a particle size of 0.5 mm in diameter (Mitsubishi, Tokyo, Japan). The purity of isolated compounds was initially assessed through thin-layer chromatography, silica gel 60 F₂₅₄ plates (Merck, NJ, USA) under UV light.

Plant Material. The whole plants of *C. fuscescens* Lindl. var. *brunnea* were obtained from the Chatuchak market in October 2019. Authentication was done by Mr. Yanyong Punpreuk, Department of Agriculture, Bangkok, Thailand. A voucher specimen (BS-CF-102562) has been placed at the Department of Pharmacognosy and Pharmaceutical Botany, Faculty of Pharmaceutical Sciences, Chulalongkorn University.

Extraction and Isolation. Dried whole plants of *C. fuscescens* Lindl. var. *brunnea* (2.3 kg) were macerated with ethanol (EtOH) (5 \times 10 L). The ethanolic extract (530 g) was mixed with water and subjected to partitioning with ethyl acetate

(EtOAc). This process yielded an ethyl acetate extract (99.2 g) and an aqueous extract (428.2 g).

The ethyl acetate extract was then separated by vacuum liquid chromatography (silica gel, EtOAc-hexane, gradient) to yield nine fractions (F1–F9). F4 (7.8 g) was subjected to further fractionation on a silica gel column (EtOAc-hexane, gradient) to yield compound 5 (50 mg). Fraction F6 (5 g) was separated on a silica gel column (EtOAc-hexane, gradient), resulting in three fractions (F6A–F6C), and fraction F6B (1 g) was then subjected to CC using an EtOAc-hexane gradient to yield three fractions (F6BA–F6BC). F6BA (150 mg) was separated again on CC (silica gel, EtOAc-hexane, gradient) to give compounds 6 (7.8 mg) and 7 (2.8 mg). F6BB (250 mg) was separated by CC (silica gel, EtOAc-hexane, and gradient) to produce compounds 8 (29.3 mg) and 9 (14 mg). F6BC (500 mg) was subjected to CC (silica gel, EtOAc-hexane, and gradient) to produce compounds 10 (37.1 mg) and 11 (120.9 mg). Fraction F7 (35 g) was fractionated on a silica gel column (EtOAc-hexane, gradient), and four fractions (F7A–F7D) were obtained. Fraction F7D (155 mg) was purified again by

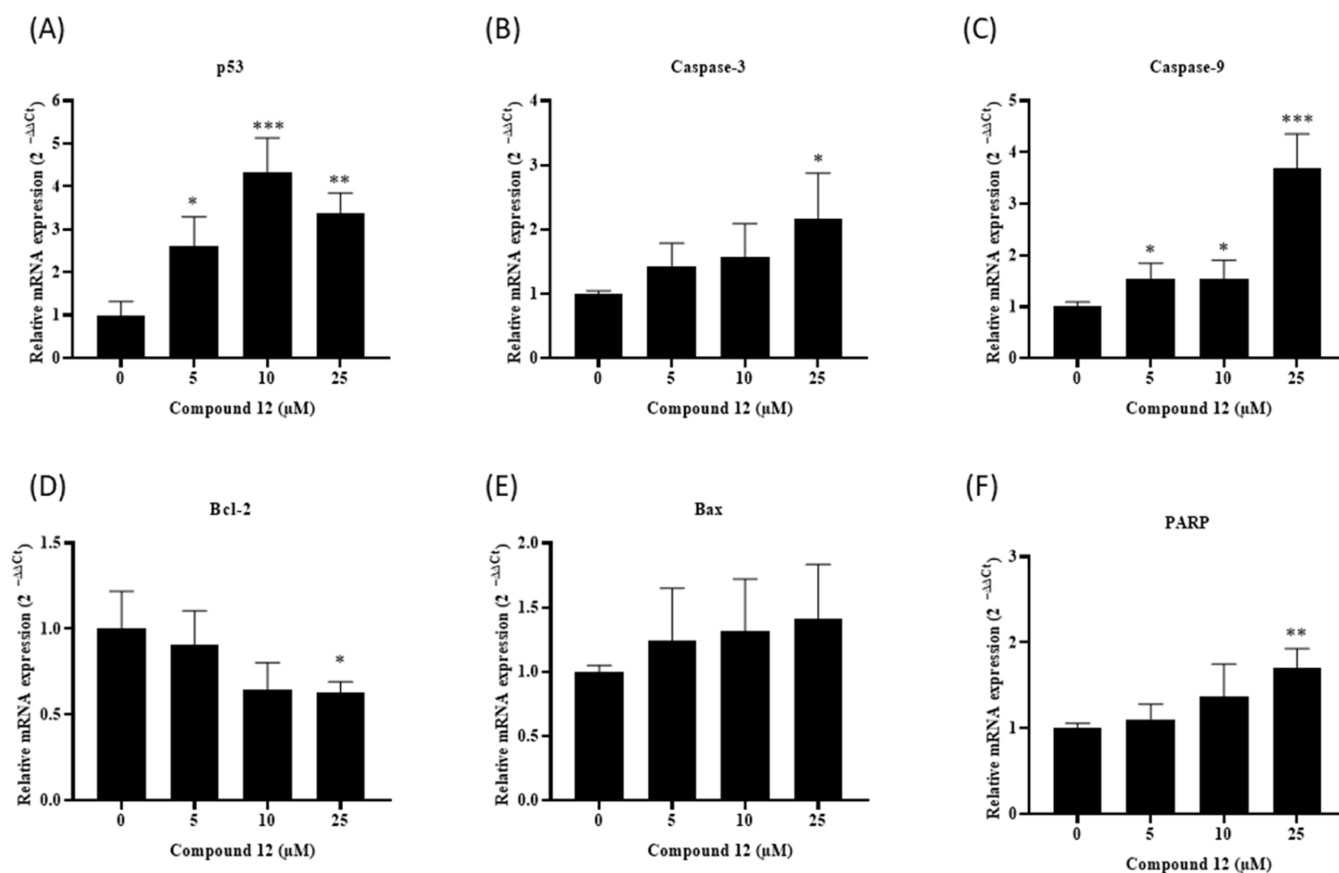


Figure 7. Investigation of the expression levels of genes related to the apoptotic pathway. p53 (A), caspase-3 (B), caspase-9 (C), Bcl-2 (D), Bax (E), and PARP (F) of compound 12-treated MDA-MB-231 cells by quantitative RT-PCR after 48 h. Data is represented as the mean \pm SD ($n = 3$) shown in common superscript as * $p \leq 0.05$, ** $p \leq 0.01$, *** $p \leq 0.001$.

Sephadex LH-20 (acetone) to give three fractions (F7D1–F7D3). Fraction F7D3 (34 mg) was then separated on silica gel (EtOH-toluene, 0.5:9.5) to furnish compound 12 (14 mg). Fraction F8 (5 g) was then separated by CC on silica gel with a gradient of EtOH–dichloromethane to yield four fractions (F8A–F8D). F8B (800 mg) was separated again by Sephadex LH-20 (acetone) to yield three fractions (F8B1–F8B3). F8B2 (300 mg) was further separated on a silica gel column (EtOH-dichloromethane, 1:9), and three fractions (F8B2A–F8B2C) were obtained. F8B2A (50 mg) was separated again by HPLC using the reverse phase (MeOH–H₂O, 1:1) to yield compound 1 (2.3 mg). F8C (450 mg) was isolated again by Sephadex LH-20 (methanol) to give four fractions (F8C1–F8C4). F8C2 (100 mg) is separated again with a silica gel column (EtOH-dichloromethane, 1:9) to yield four fractions (F8C2A–F8C2D). Compound 2 (1.9 mg) was obtained from the fraction F8C2C (30 mg) by Sephadex LH-20 (acetone). F8C3 (100 mg) was separated on CC (silica gel, EtOH-dichloromethane, 1:9) to produce four fractions (F8C3A–F8C3D). F8C3B (50 mg) was separated by Sephadex LH-20 (MeOH), and compound 4 (17.7 mg) was obtained. Separation of fraction F8D (899 mg) was done by reverse-phase column chromatography (RP-18), with gradient elution of MeOH (0–100%) in H₂O to give four fractions (F8D1–F8D4). F8D2 was separated again by Sephadex LH-20 (MeOH) to produce three fractions (F8D2A–F8D2C). F8D2B (8.5 mg) was separated by HPLC using reverse-phase (MeOH–H₂O, 1:1) and normal-phase preparative thin-layer chromatography using mobile phase (EtOH-dichloromethane, 2:8) to furnish compound 13 (3.5

mg). F8D4 (20.7 mg) was separated by CC (silica gel, EtOH-dichloromethane, and gradient) to produce three fractions (F8D4A–F8D4C). Compound 14 (3.5 mg) was obtained by purification of F8D4B (6 mg) with Sephadex LH-20 (MeOH).

The aqueous extract (428.2 mg) was separated with Diaion HP-20 (MeOH–H₂O, gradient) to give five fractions (AA–AE). Fraction AB (2 g) is separated again on a silica gel column (EtOH-dichloromethane, 3:7), and five fractions (ABA–ABE) were obtained. Compound 15 (68.4 mg) was produced by the purification of the ABE fraction (200 mg) with Sephadex LH-20 (MeOH). Fraction AC (1 g) was purified again by Sephadex LH-20 (MeOH) to give four fractions (ACA–ACD). ACB (200 mg) was separated by CC (silica gel, EtOH-dichloromethane, 3:7) to produce three fractions (ACB1–ACB3). ACB2 (36.8 mg) was subjected to semipreparative HPLC (silica gel) using the mobile phase (MeOH-dichloromethane, 1:9), and compound 3 (4.3 mg) was furnished.

Coelofuside A (1). White amorphous solid; $[\alpha]_D^{20} + 1.75$ (c 0.04, MeOH); UV (MeOH): λ_{\max} ($\log \epsilon$) 210 (4.02), 255 (4.08); HR-ESI-MS: $[M - H]^-$ at m/z : 525.1397 (calcd for C₂₇H₂₅O₁₁, 525.1396); ECD (MeOH): λ_{\max} ($\Delta\epsilon$) 201.7 (–0.27), 208.3 (+0.09), 210.9 (–0.07), 212.4 (+0.02), 215.2 (–0.06), 217.6 (+0.08) nm (Figure S10); IR: ν_{\max} at 3370, 2921, 1712, 1607, 1513, 1279, 1072 cm^{–1}.

Coelofuside B (2). White amorphous solid; $[\alpha]_D^{20} + 4.75$ (c 0.04, MeOH); UV (MeOH): λ_{\max} ($\log \epsilon$) 210 (4.32), 250 (4.40); HR-ESI-MS: $[M - H]^-$ at m/z : 433.1121 (calcd for C₂₁H₂₁O₁₀, 433.1134); ECD (MeOH): λ_{\max} ($\Delta\epsilon$) 201.8 (–0.09), 205.6 (+0.31), 210.0 (+0.19), 211.5 (–0.0002),

222.5 (−0.08), 224.5 (+0.03) nm (Figure S19); IR: ν_{\max} at 3353, 2919, 1700, 1610, 1512, 1286, 1065 cm^{-1} .

Coelofuside C (3). White amorphous solid; $[\alpha]_{\text{D}}^{20} - 1.88$ (*c* 0.08, MeOH); UV (MeOH): λ_{\max} (log ϵ) 220 (4.30), 230 (4.06), 275 (4.20); HR-ESI-MS: $[\text{M} - \text{H}]^{-}$ at *m/z*: 1033.3543 (calcd for $\text{C}_{49}\text{H}_{61}\text{O}_{24}$, 1033.3552); ECD (MeOH): λ_{\max} ($\Delta\epsilon$) 202 (+17.29), 203 (+6.87), 206 (+4.96), 209 (+4.40), 218 (+4.33), 221 (−7.97), 223 (−7.17), 225 (−6.92), 227 (−3.79) nm (Figure S3); IR: ν_{\max} at 3382, 2925, 1727, 1611, 1512, 1386, 1369, 1230, 1074 cm^{-1} .

4-O-(6'-O-Glucosyl-4"-hydroxybenzoyl)-4-hydroxybenzyl Alcohol (4). White amorphous solid; $[\alpha]_{\text{D}}^{20} - 2.75$ (*c* 0.04, MeOH); UV (MeOH): λ_{\max} (log ϵ) 210 (4.12), 230 (3.72), 260 (4.06), 314.8 (3.14); HR-ESI-MS: $[\text{M} - \text{H}]^{-}$ at *m/z*: 405.1176 (calcd for $\text{C}_{20}\text{H}_{21}\text{O}_9$, 405.1185); ECD (MeOH): λ_{\max} ($\Delta\epsilon$) 201.5 (−0.17), 203.7 (+0.14), 208.8 (+0.08), 214.9 (−0.12), 222.3 (−0.14), 227.7 (−0.11) nm (Figure S37); IR: ν_{\max} at 3347, 2919, 1700, 1608, 1513, 1284, 1071 cm^{-1} .

Cell Culture. The breast cancer cell lines T47D (human hormone-dependent breast cancer) and MDA-MB-231 (a highly aggressive, invasive, and poorly differentiated triple-negative breast cancer) as well as the human normal keratinocyte HaCaT cell line were obtained from the American Type Culture Collection (Manassas, VA, USA). Dulbecco's modified eagle Medium (Gibco, Grand Island, NY, USA) was used for culturing T47D, MDA-MB-231, and HaCaT cell lines. 10% fetal bovine serum (Merck, DA, Germany), 100 units/ml of penicillin/streptomycin (Gibco, Grand Island, NY, USA), and 2 mM L-glutamine (Gibco, Grand Island, NY, USA) were used for supplementation of the medium. The cells were cultured in a controlled environment with 5% CO_2 at a temperature of 37 °C.

Cell Viability Assay. Cell viability was evaluated by using the MTT assay. T47D, MDA-MB-231, and HaCaT cells (5×10^3 cells) were seeded into each well of a 96-well plate, and cell attachment was facilitated by an overnight incubation. Following this, the cells were treated with varying concentrations of the aqueous and ethyl acetate extracts of *C. fuscescens* Lindl. var. *brunnea* (ranging from 0 to 500 $\mu\text{g}/\text{mL}$) and for pure compounds **8**, **10**, **11**, **12**, etoposide, and carboplatin (ranging from 0 to 200 μM). The cytotoxicity assay was performed after 48 h. Post-treatment, the cells were exposed to 100 μL of the MTT solution for 4 h at 37 °C. The absorbance of the resulting MTT product was assessed at 570 nm using a microplate reader. The percentage of viable cells was determined to be relative to the control cells.

Cell Death Evaluation. The level of apoptotic and necrotic cell death was assessed through costaining with Hoechst 33342 and PI. Following the treatments, cells were stained with 10 $\mu\text{g}/\text{mL}$ Hoechst and 5 $\mu\text{g}/\text{mL}$ PI for 30 min at 37 °C and then observed. The images of cells were obtained using fluorescence microscopy. (Olympus IX 51 with DP70; Olympus, Tokyo, Japan).

Extraction of RNA from Cells. The cells were seeded and grown for 24 h. Subsequently, the cells were exposed to oxoflavin (0–25 μM) which is the IC_{50} of the MDA-MB-231 cell lines. Ribonucleic acid (RNA) was extracted by centrifuging the cells with 500 μL of phosphate-buffered saline at 3,000 rpm for 5 min, then adding TRIzol reagent solution with volume 1000 μL , mixing and leaving at 4 °C for 5 min, and then adding 200 μL of chloroform and leaving at room temperature 5 min. Following this, the sample was centrifuged at 12,000 rpm for 15 min at 4 °C. The RNA molecule layer was separated into a colorless upper aqueous layer, placed in a 1.5 mL Eppendorf

tube, and 500 μL of 100% isopropanol, incubated at room temperature for 10 min, and then centrifuged at 12,000 rpm for 15 min at a temperature of 4 °C. After that, the supernatant was poured to get the RNA pellet. 75% Ethanol (500 μL) was used to wash the RNA pellet and then centrifuged at 10,000 rpm for 5 min at 4 °C for two cycles. Then, the RNA pellet was left to dry for 15 min and then resuspend. With DEPC water, volume 50 μL , the concentration (concentration) and purity (purification) of RNA molecules extracted were measured with Nanodrop and a bioanalyzer. Extracted RNA samples can be stored in a −80 °C freezer.

Quantitative Real-Time PCR. qPCR reaction mixture consisted of 0.5 μL of the products of the RT reaction, 0.4 μL of forward primer (10 μM), 0.4 μL of reverse primer (10 μM), 10 μL of SYBR qPCR SuperMix, and 8.7 μL of nuclease-free H_2O to achieve a total volume of 20 μL . The qPCR reaction involved denaturation at 95 °C for 30 s, following 45 cycles of 95 °C for 5 s and 58 °C for 35 s using a real-time thermal cycler (7500 Real-Time PCR System; Applied Biosystems, Thermo Fisher Scientific). Negative controls included no template reactions. Product specificity in real-time PCR was confirmed through melting curve analysis, gel electrophoresis, and sequencing. GAPDH was used as endogenous control gene, and the messenger RNA level in MDA-MB-231 cells treated with oxoflavin was normalized to that of untreated control using the $2^{-\Delta\Delta\text{CT}}$ method.

List of primers for quantitative RT-PCR

1. Bcl-2—FW: GATAACGGAGGCTGGGATGC, RV: TCCTTGTGGCCAGATAGG
2. Bax—FW: AAAGTGGTGCTCAAGGCC, RV: CTTCACTGACTCGGCCAGG
3. Caspase-3—FW:GAGCCATGGTGAAGAAGGAA-TA, RV: TCAATGCCACAGTCCAGTTC
4. Caspase-9—FW: CGACCTGACTGCCAAGAAA, RV: CATCCATCTGTGCCGTAGAC
5. PARP—FW: AGCACAGTGCGGATTCTGTGTC, RV: ACCGTTGTTGACCTCACAGT
6. p53—FW: GAGATGTTCCGAGAGCTGATG, RV: TTTATGGCGGGAGGTAGACT
7. Gapdh—FW: TTCAGCTCAGGGATGACCTT
8. Gapdh—RV: ACCCAGAAGACTGTGGATGG

Statistical Analysis. GraphPad Prism Version 8 was employed for the analysis of all data. Data were presented as the mean \pm SD, and the analysis was based on at least three independent experiments. Statistical analyses were conducted using one-way analysis of variance, followed by Tukey's post hoc test, with a significance level set at $p < 0.05$.

■ ASSOCIATED CONTENT

Supporting Information

The Supporting Information is available free of charge at <https://pubs.acs.org/doi/10.1021/acsomega.3c07048>.

HR-ESI-MS spectra; UV spectra; FT-IR spectra of compounds **1–4**; 1D and 2D NMR of compounds **1–15**; CD spectra of compounds **1, 2, 4, 13, and 14**; and IC_{50} values of compounds **8, 10, 11, 12**, etoposide, and carboplatin against the T47D and MDA-MB-231 breast cancer cell lines and the HaCaT human keratinocyte (PDF)

AUTHOR INFORMATION

Corresponding Author

Boonchoo Sritularak – Department of Pharmacognosy and Pharmaceutical Botany, Faculty of Pharmaceutical Sciences and Natural Products for Ageing and Chronic Diseases Research Unit, Faculty of Pharmaceutical Sciences, Chulalongkorn University, Bangkok 10330, Thailand; orcid.org/0000-0001-8352-4122; Email: boonchoo.sr@chula.ac.th

Authors

May Thazin Thant – Department of Pharmacognosy and Pharmaceutical Botany, Faculty of Pharmaceutical Sciences, Chulalongkorn University, Bangkok 10330, Thailand
Narumol Bhummaphan – College of Public Health Sciences, Chulalongkorn University, Bangkok 10330, Thailand
Jittima Wuttiin – Department of Pharmacognosy and Pharmaceutical Botany, Faculty of Pharmaceutical Sciences, Chulalongkorn University, Bangkok 10330, Thailand
Charoenchai Puttipanyalears – Department of Anatomy, Faculty of Medicine, Chulalongkorn University, Bangkok 10330, Thailand
Waraluck Chaichompoo – Department of Food and Pharmaceutical Chemistry, Faculty of Pharmaceutical Sciences and Natural Products for Ageing and Chronic Diseases Research Unit, Faculty of Pharmaceutical Sciences, Chulalongkorn University, Bangkok 10330, Thailand
Pornchai Rojsitthisak – Department of Food and Pharmaceutical Chemistry, Faculty of Pharmaceutical Sciences and Natural Products for Ageing and Chronic Diseases Research Unit, Faculty of Pharmaceutical Sciences, Chulalongkorn University, Bangkok 10330, Thailand; orcid.org/0000-0001-5991-1843
Yanyong Punpreuk – Department of Agriculture, Ministry of Agriculture and Cooperatives, Bangkok 10900, Thailand
Chotima Böttcher – Experimental and Clinical Research Center, a Cooperation Between the Max Delbrück Center for Molecular Medicine in the Helmholtz Association, Charité—Universitätsmedizin Berlin, Berlin 13125, Germany
Kittisak Likhitwitayawuid – Department of Pharmacognosy and Pharmaceutical Botany, Faculty of Pharmaceutical Sciences, Chulalongkorn University, Bangkok 10330, Thailand

Complete contact information is available at:

<https://pubs.acs.org/10.1021/acsomega.3c07048>

Notes

The authors declare no competing financial interest. During the preparation of this work, the author(s) used GPT-3.5 and Bard AI in order to assist in the writing process. After using this tool/service, the author(s) reviewed and edited the content as needed and take full responsibility for the content of the publication.

ACKNOWLEDGMENTS

M.T.T. is grateful to Chulalongkorn University for a C2F (Second Century Fund) postdoctoral fellowship under the supervision of B.S.

REFERENCES

- (1) Dash, S. L.; Mohapater, R.; Mishra, S. K. Anticancer activity study of some selected Indian medicinal plants used traditionally. *J. Pharm. Negative Results* **2023**, *14*, 125–132.
- (2) Arnold, M.; Morgan, E.; Rungay, H.; Mafra, A.; Singh, D.; Laversanne, M.; Vignat, J.; Gralow, J. R.; Cardoso, F.; Siesling, S.; Soerjomataram, I. Current and future burden of breast cancer: Global statistics for 2020 and 2040. *Breast* **2022**, *66*, 15–23.
- (3) Tuli, H. S.; Garg, V. K.; Bhushan, S.; Uttam, V.; Sharma, U.; Jain, A.; Sak, K.; Yadav, V.; Lorenzo, J. M.; Dhama, K.; Behl, T.; et al. Natural flavonoids exhibit potent anticancer activity by targeting microRNAs in cancer: A signature step hinting towards clinical perfection. *Transl. Oncol.* **2023**, *27*, 101596.
- (4) Śliwiński, T.; Kowalczyk, T.; Sitarek, P.; Kolanowska, M. Orchidaceae-derived anticancer agents: A review. *Cancers* **2022**, *14*, 754.
- (5) Thitikornpong, W.; Jithavech, P.; Thompho, S.; Punpreuk, Y.; Halim, H.; Sritularak, B.; Rojsitthisak, P. Development and validation of a simple, sensitive and reproducible method for simultaneous determination of six polyphenolic bioactive markers in *Dendrobium* plants. *Arabian J. Chem.* **2022**, *15*, 104038.
- (6) Jimoh, T. O.; Costa, B. C.; Chansrinoyom, C.; Chaotham, C.; Chanvorachote, P.; Rojsitthisak, P.; Likhitwitayawuid, K.; Sritularak, B. Three new dihydrophenanthrene derivatives from *Cymbidium ensifolium* and their cytotoxicity against cancer cells. *Molecules* **2022**, *27*, 2222.
- (7) Jimoh, T. O.; Nuamnaichati, N.; Sungthong, R.; Chansrinoyom, C.; Chanvorachote, P.; Likhitwitayawuid, K.; Chaotham, C.; Sritularak, B. Phytochemicals from *Vanda bensonii* and their bioactivities to inhibit growth and metastasis of non-small cell Lung cancer cells. *Molecules* **2022**, *27*, 7902.
- (8) Kosavitkul, P. Species diversity of wild orchids of Nan province. *NUJST* **2010**, *18*, 46–54.
- (9) Koirala, D.; Pradhan, S.; Pant, B. A symbiotic seed germination and plantlet development of *Coelogyne fuscescens* Lindl., a medicinal orchid of Nepal. *Sci. World* **2013**, *11*, 97–100.
- (10) Koirala, D. R. In Vitro Seed Germination of *Cymbidium Aloifolium* (L.) SW. and micropropagation of *Coelogyne fuscescens* Lindl. by tissue culture technique. Doctoral dissertation, Department of Botany, Tribhuvan University, Nepal, 2007, 5.
- (11) Teoh, E. S. Medicinal orchids of Thailand and Myanmar. In *Orchids as aphrodisiac, medicine or food*; Springer Nature Switzerland AG, 2019; pp 245–254.
- (12) Wen, L.; Weiming, C.; Zhi, X.; Xiaotain, L. New triterpenoids of *Pholidota chinensis*. *Planta Med.* **1986**, *52*, 4–6.
- (13) Guo, X.-Y.; Wang, J.; Wang, N.-L.; Kitataka, S.; Liu, H.-W.; Yao, X.-S. New stilbenoids from *Pholidota yunnanensis* and their inhibitory effects on nitric oxide production. *Chem. Pharm. Bull.* **2006**, *54*, 21–25.
- (14) Kalinowska, M.; Świsłocka, R.; Lewandowski, W. The spectroscopic (FT-IR, FT-Raman and ¹H, ¹³C NMR) and theoretical studies of cinnamic acid and alkali metal cinnamates. *J. Mol. Struct.* **2007**, *834–836*, 572–580.
- (15) Majumder, P. L.; Datta, N.; Sarkar, A. K.; Chakraborti, J. Flavidin. A novel 9,10 dihydrophenanthrene derivative of the orchids *Coelogyne flvida*, *Pholidota articulata* and *Otochilus fusca*. *J. Nat. Prod.* **1982**, *45*, 730–732.
- (16) Lee, M.; Lee, D. G.; Lee, K. H.; Cho, S. H.; Nam, K. W.; Lee, S. Isolation and identification of phytochemical constituents from the fruits of *Acanthopanax senticosus*. *Afr. J. Pharm. Pharmacol.* **2013**, *7*, 294–301.
- (17) Rueda, D. C.; Schöffmann, A.; De Mieri, M.; Raith, M.; Jähne, E. A.; Hering, S.; Hamburger, M. Identification of dihydrostilbenes in *Pholidota chinensis* as a new scaffold for GABAA receptor modulators. *Bioorg. Med. Chem.* **2014**, *22*, 1276–1284.
- (18) Syafni, N.; Putra, D. P.; Arbain, D. 3,4-Dihydroxybenzoic acid and 3,4-dihydroxybenzaldehyde from the fern *Trichomanes chinense* L.; isolation, antimicrobial and antioxidant properties. *Indones. J. Chem.* **2012**, *12*, 273–278.
- (19) Majumder, P. L.; Datta, N. Structure of oxoflavin, a 9, 10-dihydrophenanthropyron from *Coelogyne elata*. *Phytochemistry* **1984**, *23*, 671–673.
- (20) Zidorn, C.; Ellmerer-Müller, E. P.; Stuppner, H. A germacranolide and three hydroxybenzyl alcohol derivatives from

Hieracium murorum and *Crepis bocconi*. *Phytochem. Anal.* **2001**, *12*, 281–285.

(21) Lee, K. H.; Tagahara, K.; Suzuki, H.; Wu, R. Y.; Haruna, M.; Hall, I. H.; Huang, H. C.; Ito, K.; Iida, T.; Lai, J. S. Antitumor agents. 49. Tricin, kaempferol-3-*O*- β -D-glucopyranoside and (+)-nortrachelogenin, antileukemic principles from *Wikstroemia indica*. *J. Nat. Prod.* **1981**, *44*, 530–535.

(22) Cota, B. B.; Magalhães, A.; Pimenta, A.; Siqueira, E. P.; Alves, T.; Zani, C. L. Chemical constituents of *Habenaria petalodes* Lindl. (Orchidaceae). *J. Braz. Chem. Soc.* **2008**, *19*, 1098–1104.

(23) Morikawa, T.; Xie, H.; Matsuda, H.; Yoshikawa, M. Glucosyloxybenzyl 2-isobutylmalates from the tubers of *Gymnadenia conopsea*. *J. Nat. Prod.* **2006**, *69*, 881–886.

(24) Huang, S. Y.; Li, G. Q.; Shi, J. G.; Mo, S. Y.; Wang, S. J.; Yang, Y. C. Chemical constituents of the rhizomes of *Coeloglossum viride* var. *bracteatum*. *J. Asian Nat. Prod. Res.* **2004**, *6*, 49–61.

(25) Han, S. W.; Wang, X. J.; Cui, B. S.; Sun, H.; Chen, H.; Ferreira, D.; Li, S.; Hamann, M. T. Hepatoprotective glucosyloxybenzyl 2-hydroxy-2-isobutylsuccinates from *Pleione yunnanensis*. *J. Nat. Prod.* **2021**, *84*, 738–749.

(26) Kizu, H.; Kaneko, E. I.; Tomimori, T. Studies on nepalese crude drugs. XXVI. Chemical constituents of *Panch Aunle*, the roots of *Dactylorhiza hatagirea* D. Don. *Chem. Pharm. Bull.* **1999**, *47*, 1618–1625.

(27) Singh, A.; Duggal, S. Medicinal orchids—an overview. *Ethnobotanical Leaflet*. **2009**, *13*, 399–412.

(28) Jaiswal, R.; Kuhnert, N. Identification and characterization of the phenolic glycosides of *Lagenaria siceraria* Stand. (Bottle Gourd) fruit by liquid chromatography-tandem mass spectrometry. *J. Agric. Food Chem.* **2014**, *62*, 1261–1271.

(29) Guiro, K.; Patel, S. A.; Greco, S. J.; Rameshwar, P.; Arinze, T. L. Investigating breast cancer cell behavior using tissue engineering scaffolds. *PLoS One* **2015**, *10*, No. e0118724.

(30) Giannone, G.; Milani, A.; Ghisoni, E.; Genta, S.; Mittica, G.; Montemurro, F.; Valabrega, G. Oral etoposide in heavily pre-treated metastatic breast cancer: A retrospective series. *Breast* **2018**, *38*, 160–164.

(31) Phung, H. M.; Lee, H.; Lee, S.; Jang, D.; Kim, C. E.; Kang, K. S.; Seo, C. S.; Choi, Y. K. Analysis and anticancer effects of active compounds from *Spatholobi caulis* in human breast cancer cells. *Processes* **2020**, *8*, 1193.

(32) Vousden, K.; Prives, C. Blinded by the light: the growing complexity of p53. *Cell* **2009**, *137*, 413–431.

(33) Alshatwi, A. A.; Subash-Babu, P.; Antonisamy, P. Violacein induces apoptosis in human breast cancer cells through up regulation of BAX, p53 and down regulation of MDM2. *Exp. Toxicol. Pathol.* **2016**, *68*, 89–97.

(34) Kong, C. S.; Kim, J. A.; Yoon, N. Y.; Kim, S. K. Induction of apoptosis by phloroglucinol derivative from *Ecklonia cava* in MCF-7 human breast cancer cells. *Food Chem. Toxicol.* **2009**, *47*, 1653–1658.

(35) Li, P.; Nijhawan, D.; Budihardjo, I.; Srinivasula, S. M.; Ahmad, M.; Alnemri, E. S.; Wang, X. Cytochrome c and dATP-dependent formation of Apaf-1/caspase-9 complex initiates an apoptotic protease cascade. *Cell* **1997**, *91*, 479–489.

(36) Balachandran, C.; Emi, N.; Arun, Y.; Yamamoto, Y.; Ahilan, B.; Sangeetha, B.; Duraipandiyan, V.; Inaguma, Y.; Okamoto, A.; Ignacimuthu, S.; et al. In vitro anticancer activity of methyl caffeate isolated from *Solanum torvum* Swartz. fruit. *Chem.-Biol. Interact.* **2015**, *242*, 81–90.